Available online at www.sciencedirect.com
SCIENCE DIRECT®
Optics Communications 241 (2004) 449–454
OPTICS COMMUNICATIONS
www.elsevier.com/locate/optcom

Passive mode locking of a Cr^{4+}:YAG laser by PbS quantum-dot-doped glass saturable absorber

A.A. Lagatsky [a,*], C.G. Leburn [a], C.T.A. Brown [a], W. Sibbett [a], A.M. Malyarevich [b], V.G. Savitski [b], K.V. Yumashev [b], E.L. Raaben [c], A.A. Zhilin [c]

[a] *J.F. Allen Physics Research Laboratories, School of Physics and Astronomy, University of St. Andrews, North Haugh, St. Andrews KY16 9SS, Scotland, UK*
[b] *International Laser Center, 65 F. Skaryna Avenue, 220013 Minsk, Belarus*
[c] *S.I. Vavilov State Optical Institute, St. Petersburg, Russia*

Received 24 April 2004; received in revised form 29 June 2004; accepted 8 July 2004

Abstract

The use of PbS quantum-dot-doped glass as an intracavity saturable absorber for passive mode locking of a Cr^{4+}:YAG laser was investigated. We obtained 10 ps pulses at a repetition rate of 235 MHz with an average output power of 35 mW. This mode-locked laser was tunable from 1460 to 1550 nm.

PACS: 42.55.Rz; 42.60.Fc; 42.70.Hj
Keywords: Laser; Mode-locking; Solid-state; Saturable absorber

1. Introduction

There is a continued interest in the development of novel optical materials with saturable absorption properties for the passive mode locking of lasers. Using a range of approaches, this technique enables ultrashort pulse generation in a number of solid-state lasers [1]. These advances are significant because reliable, compact and efficient mode-locked lasers are finding increasingly wide applications in ultrafast measurements, biomedical imaging and telecommunications studies. Several types of the materials have been used as saturable absorbers for mode locking in solid-state lasers that operate in the near-IR spectral region. Epitaxially grown bulk and quantum well semiconductor

* Corresponding author. Tel.: +44-1334-463-053; fax: +44-1334-463-104.
E-mail address: aal2@st-andrews.ac.uk (A.A. Lagatsky).

0030-4018/$ - see front matter
doi:10.1016/j.optcom.2004.07.022

saturable absorber mirrors (SESAMs) [2] and saturable Bragg reflectors (SBRs) [3] represent those most commonly used to date. Such structures possess appropriate absorption saturation fluences and recovery times, as well as sufficiently broad bandwidth characteristics for ultrashort pulse operation and they can be incorporated into appropriate resonator designs. However, the molecular beam epitaxial growth technique is relatively demanding and expensive and it also requires specific lattice matching conditions to be satisfied such that there are limitations in the choice of semiconductor materials to cover the spectral ranges of modern lasers. Non-epitaxially grown semiconductor doped silica films have been demonstrated for solid-state laser mode locking [4–6]. Thin films of InAs semiconductor microcrystalites in silica were fabricated using a radio-frequency sputtering technology which offers flexibility in the choice of semiconductor dopant and substrate material. However, a relatively high saturation fluence of these absorbers ($\sim$10 mJ/cm^2) makes them difficult to use for direct saturable-absorber mode locking (without Kerr-lens mode locking) in solid-state lasers.

Semiconductor-doped glasses offer attractive characteristics as solid-state saturable absorbers. Firstly, they can be fabricated using a simpler and low cost batch-melting technique. Secondly, variation of the nanocrystal size leads to a change of the spectral position of the excitonic absorption peak. This means that a single semiconductor material facilitates saturable absorption over a substantial spectral region simply through this variation in the size of nanocrystals. The glasses doped with CdTe nanoparticles have been used as a saturable absorbers for passive mode locking of a Ti:Sapphire laser in the 780–860 nm range [7,8]. Lead sulphide (PbS) is a IV–VI type semiconductor with band gap of 0.41 eV and exciton Bohr radius of 18 nm [9]. Such the large exciton Bohr radius implies that in crystallites that are several nanometers in size there will be a strong quantum confinement of the electrons and holes. This quantum confinement in PbS nanocrystals (or quantum dots) manifests itself as a pronounced blue shift of the energy bandgap and an enhancement of nonlinearity in the range of the lowest in energy absorption transition (first excitonic resonance) [10]. When the PbS quantum dots (PbS QDs) range in size from 2 to 7 nm the bandgap changes mean that the absorption resonances are shifted from 1 to 2.5 μm [11]. Using such structures passive mode locking in cw Cr:forsterite laser [12,13] and pulsed neodymium lasers [14–16] was demonstrated at centre operating wavelengths around 1.3 and 1 μm, respectively.

In this communication, we report results where a PbS QD-doped glass has been used as a saturable absorber for the passive mode-locking of a cw Cr^{4+}:YAG laser operating around 1.5 μm. The tuning range of this laser overlapped conveniently the third optical communications window.

2. Optical properties of the PbS-doped glass

Our silicate glass sample was prepared from a SiO_2–Al_2O_3–NaF–Na_2O–ZnO glass system. The compositions and technological regimes (temperature, time and reducing conditions) were developed for the synthesis of the initial series of colorless silicate glass samples with a maximal semiconductor concentration of 0.4–0.6 mol.%. A double-stage process of heat-treatment allowed a required volume of PbS crystalline fraction with a pre-determined dot size to be obtained. The first stage in this process is a prolonged low-temperature treatment for PbS nucleation (480 °C, 72 h). This was followed by the nanocrystals growth phase that was performed at 520 °C for a period of 25 h. The correlation between time-temperature heat-treatment regimes and the location of the first excitonic resonance of the PbS QDs was found by the analysis of small-angle X-ray scattering (SAXS) data (scattering by monodispersed spherical particles assumed). Fig. 1 shows the room-temperature absorption spectrum of PbS QDs-doped glass sample (referred to below as PbS-doped glass) that was assessed in this work. The first excitonic peak is at 1.4 μm and the average dot diameter is estimated to be 5.4 nm.

In Fig. 2 the relaxation time characteristics for the PbS-doped glass sample are indicated. To obtain this measurement, 15-ps pulses from passively mode-locked Nd:$YAlO_3$ laser (λ = 1.08 μm) were

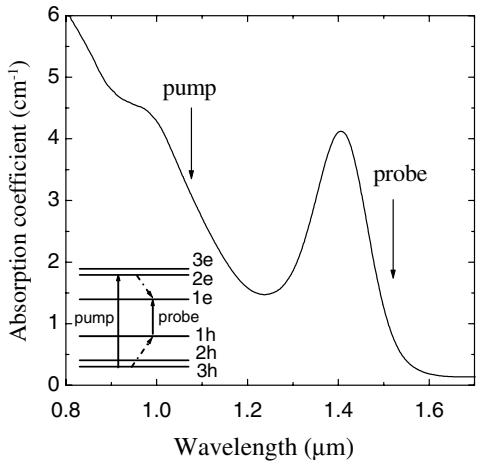

Fig. 1. Room-temperature absorption spectrum of the silicate glass doped with PbS QDs. Inset is the energy-level diagram for PbS QDs, where the subscripts e and h denote electron and hole quantum confined energy levels, respectively. Following to [6], 1e denotes $|j = 1/2, \pi = -1\rangle$ state, 2e – $|j = 3/2, \pi = 1\rangle$, 3e – $|j = 1/2, \pi = 1\rangle$, 1h – $|j = 1/2, \pi = 1\rangle$, 2h – $|j = 3/2, \pi = -1\rangle$, and 3h – $|j = 1/2, \pi = -1\rangle$.

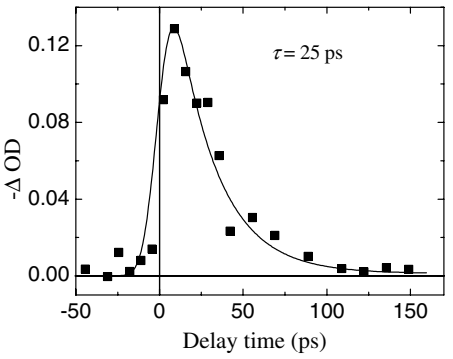

Fig. 2. Kinetics of bleaching relaxation for PbS-doped glass at 1.524 μm after pump at 1.08 μm. Solid line – result of the best fit to the experimental data (squares).

used as the optical excitation. The third Raman Stokes (λ = 1.524 μm, which corresponded to 901 cm^{-1} of frequency shift) from a $KGd(WO_4)_2$ crystal, excited by an intensity component of the laser pulse, was used as a probe pulse. The pump pulse had a diameter of 3 mm giving the pump intensity on the sample of ~1 GW/cm^2 (~15 mJ/cm^2). The bleaching value was defined as the differential absorption $\Delta OD = -\log(T/T_0)$, where T_0 and T are the transmissions of the probe beam without and with pump beam present, respectively. It should be noted that the 1.08-μm pump excites a group of higher energy excitonic transitions in QDs which is observable as a pronounced shoulder feature in the absorption spectrum in the vicinity of 1 μm (see Fig. 1). Following pumping, the excited electrons and holes relax from the pumped energy levels to the lowest in energy states (corresponding to the 1.4 μm transition) at sub-picosecond timescales [13,17]. The characteristic time of this relaxation process is much shorter than the 15 ps duration of the pump pulses and so this was not be resolved. Bleaching at 1.5 μm is caused by a state-filling effect due to the occupation by electrons and holes of their lowest in energy excited states. Direct carrier recombination or carrier relaxation through the defect states of the QDs leads to the bleaching relaxation kinetics as indicated in Fig. 2. The process of bleaching relaxation in PbS QDs in the range of the first excitonic resonance has previously been shown to take the form of a double exponential [13,15]. The ratio of fast and slow amplitudes A_f/A_s varies along the shape of the first excitonic absorption band [15], so that a narrow wavelength interval exists where the impact of the slow component is negligible (of the order of a few percent). For a saturable absorber intended for use as a passive mode-locking element, fast bleaching relaxation is desirable and so the sample studied here was chosen to satisfy this requirement. A double-exponential fit to the experimental data (solid line in the Fig. 2) while taking pump and probe pulse durations into account implies a value of 25 ± 3 ps for the fast relaxation component. The ratio A_s/A_f is 0.05 which indicates that the slow bleaching relaxation component is not considerable for this PbS-doped glass.

Absorption saturation measurements of the PbS-doped glass were performed at 1.34 μm using a passively Q-switched Nd:$YAlO_3$ laser that produced 40 ns pulses. The pump beam was focused into a spot of 250 μm in diameter providing an energy fluence on the sample of up to 10 J/cm^2. Fig. 3 shows the intensity-dependent transmission (squares) of the PbS-doped glass at 1.34 μm. The intensity-dependent absorption, α, is modeled within the frame of a two-level scheme for a fast

saturable absorber. For a pump pulse that is much longer than the bleaching relaxation time of the saturable absorber having a non-saturable absorption coefficient of α_{ns}, then

$$\alpha = \frac{\alpha_0}{1 + I/I_{sat}} + \alpha_{ns}, \quad (1)$$

where α_0 is the saturable absorption coefficient, I is the input intensity and I_{sat} is the saturation intensity. The best fit is shown by the solid line in Fig. 3. The saturable absorber parameters were thus estimated to be: $\alpha_0/\alpha_{ns} = 2.4$, $I_{sat} = 8$ MW/cm^2. The non-saturable absorption includes the excited state absorption from the lowest energy excitonic state. Using the above values it was possible to estimate ground-state absorption cross-section as well as saturation fluence for the PbS-doped glass. Assuming that the relaxation time at the wavelength 1.34 μm has the same value as at 1.52 μm ($\tau = 25$ ps) the ground-state absorption cross-section at 1.34 μm can be estimated as follows: $\sigma_{gsa} = h\nu/I_{sat}\tau \approx 7 \times 10^{-16}$ cm^2. From the absorption spectrum (Fig. 1) the ground-state absorption cross-section at 1.51 μm can be calculated to be $\sigma_{gsa} \approx 3 \times 10^{-16}$ cm^2. Therefore, the saturation fluence at the wavelength of 1.51 μm is evaluated as $F_{sat} = h\nu\sigma_{gsa} \approx 500$ μJ/cm^2. It is known that for SESAMs of different designs the saturation fluence value F_{sat} varies in the range from ~10 to 100 μJ/cm^2 [2,18].

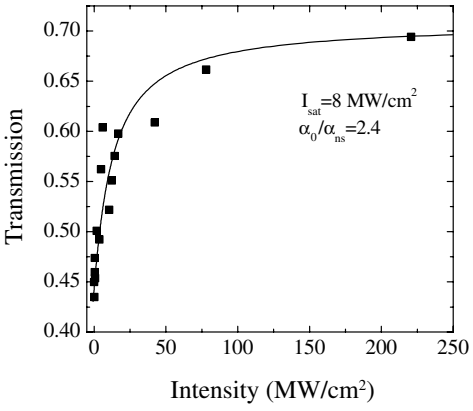

Fig. 3. Intensity-dependent transmission of PbS-doped glass at 1.34 μm. Solid line – result of the best fit to the experimental data (squares) in the frame of the two-level model of the fast-relaxing saturable absorber.

3. Passive mode-locking of a cw Cr:YAG laser by the PbS-doped glass

For the laser experiments reported here we designed a highly asymmetric four-mirror resonator for the Cr:YAG laser (Fig. 4). The pump source was a 10 W, Yb-doped fiber laser operating at 1064 nm. The Cr:YAG crystal was a Brewster-cut 20 mm long cylindrical rod and was placed between two high reflectivity folding mirrors for tight focussing. For optimised cw operation and subsequent adaptation to passive mode locking, the long arm of the cavity was set to ~40 cm and the short arm varied in the range between 50 and 100 mm. A beam waist in the range of 12–60 μm was formed at the end of short arm. During cw operation, the Cr:YAG laser gave a maximum output powers of 650 and 980 mW at 1490 nm with 0.5% and 1% output coupling, respectively, and the laser output could be tuned from 1400 to 1580 nm.

For incorporation as a saturable absorber in the laser cavity, the PbS-doped glass plate was polished to a thickness of 90 μm and AR-coated for wavelengths centered on 1500 nm. The small-signal absorption of the sample ranged from 3% to 0.3% over the 1450–1550 nm region. Self-starting mode-locked operation of the laser was obtained when the glass sample was inserted in contact with the HR mirror in the short arm of the cavity where the beam waist was 20 μm. A 235 MHz sequence

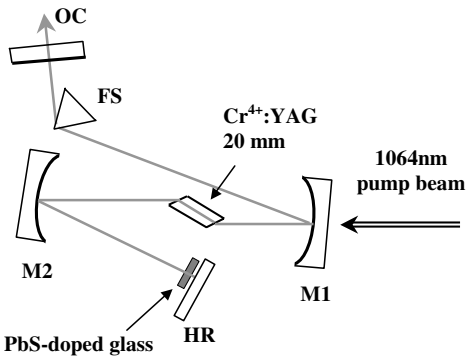

Fig. 4. Schematic of the Cr:YAG laser: M1, concave high reflector mirror ($R = 100$ mm); M2, concave high reflector mirror ($R = 75$ mm); FS, fused-silica prism; OC, 0.5% output coupler; HR, high reflector.

of pulses with average output power of 35 mW was obtained for a pump power of 6 W. Assuming $sech^2$ intensity profiles, the pulse duration was deduced from autocorrelation measurements to be 10 ps. For the observed spectral width of 0.3 nm at a center wavelength of 1509.5 nm, the implied duration-bandwidth product was 0.4 (Fig. 5). Stable mode-locked operation was observed when the PbS-doped glass plate was placed within 1 mm of the high reflectivity mirror such that the laser mode radius varied in from 20 to 31 μm corresponding to intensities on the saturable absorber of 0.2–0.1 GW/cm^2. Mode locking was maintained throughout the day-long operational period implying that photodarkening in the QD-doped glass was not present.

It was possible to tune the laser during mode-locking operation from 1460 to 1550 nm (Fig. 6). Tuning was accomplished by a fused-silica prism. The tunability to the shorter wavelength region was limited by an increase in the absorption of the saturable absorber. An absence of mode-locking operation at wavelengths longer than 1550 nm can be accounted for by the decrease in the modulation depth of the saturable absorber. The relatively low efficiency of the laser during mode-locked operation can be explained by presence of additional intracavity losses due to the relatively poor AR-coating of the glass plate and the non-saturable absorption in the PbS-doped glass structure. The poor AR coating is not related to the particular type of PbS-doped glass studied here, and can be improved by using better AR coating workmanship.

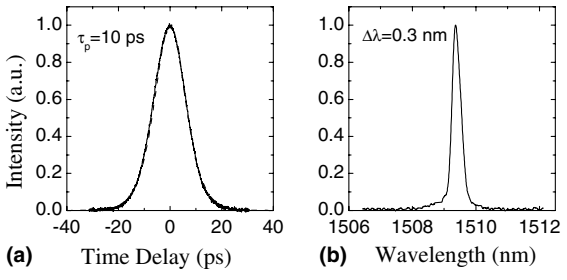

Fig. 5. Intensity autocorrelation (a), dotted curve is fit assuming an ideal $sech^2$ pulseshape, and spectrum (b) of mode-locked pulses from the Cr:YAG laser.

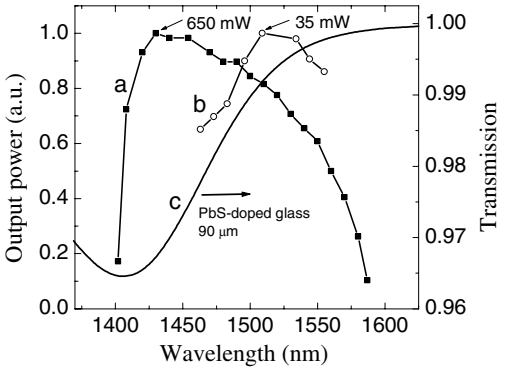

Fig. 6. Tunability of the Cr:YAG laser during cw (a) and mode-locked operation (b). Curve c is transmission spectrum of the PbS QD-doped glass saturable absorber.

4. Conclusions

In conclusion, a new saturable absorber based on PbS QD-doped silicate glass has been demonstrated for the passive mode-locking of a cw Cr:YAG laser. The kinetics of the bleaching relaxation for PbS-doped glass around 1.5 μm were measured and this revealed a fast relaxation component of 25 ps. With a highly asymmetric, four-mirror resonator 10 ps pulses were obtained with an output average power of 35 mW centered at 1509 nm at a repetition rate of 235 MHz. In the mode-locking regime the laser was tunable from 1460 to 1550 nm. It has to be acknowledged that these results do not compete on pulse duration with those obtained from the femtosecond Cr:YAG lasers with SESAM structures for the passive mode-locking, where sub-100 fs pulses have been generated [19,20]. However, it is expected that significantly more impressive results with increased average output powers and reduced pulse durations will be possible by further optimisation of the QD-doped glass saturable absorber element and its controllable parameters.

Acknowledgement

The authors thank the Royal Society, UK, for funding through the Royal Society-Belarus–UK Joint Grant.

References

[1] U. Keller, Nature 424 (2003) 831.
[2] U. Keller, K.J. Weingarten, F.X. Kärtner, D. Kopf, B. Braun, I.D. Jung, R. Fluck, C. Hönninger, N. Matuschek, J. Aus der Au, IEEE J. Select. Top. Quantum Electron. 2 (1996) 435.
[3] S. Tsuda, W.H. Knox, S.T. Cundiff, W.Y. Jan, J.E. Cunningham, IEEE J. Select. Top. Quantum Electron. 2 (1996) 454.
[4] I.P. Bilinsky, J.G. Fujimoto, J.N. Walpole, L.J. Missaggia, Appl. Phys. Lett. 74 (1999) 2411.
[5] I.P. Bilinsky, J.G. Fujimoto, J.N. Walpole, L.J. Missaggia, Opt. Lett. 23 (1998) 1766.
[6] R.P. Prasankumar, C. Chudoba, J.G. Fujimoto, P. Mak, M.F. Ruane, Opt. Lett. 27 (2002) 1564.
[7] N. Sarukura, Y. Ishida, T. Yanagawa, H. Nakano, Appl. Phys. Lett. 57 (1990) 229.
[8] I.P. Bilinsky, R.P. Prasankumar, J.G. Fujimoto, JOSA B 16 (1999) 546.
[9] Landolt-Bornstein, in: O. Madelung (Ed.), New Series, vol. 17, subvol. F, Springer, New York, 1983, p. 155.
[10] A.D. Yoffe, Adv. Phys. 42 (1993) 173.
[11] I. Kang, F.W. Wise, JOSA B 14 (1997) 1632.
[12] P.T. Guerreiro, S. Ten, N.F. Borrelli, J. Butty, G.E. Jabbour, N. Peyghambarian, Appl. Phys. Lett. 71 (1997) 1595.
[13] K. Wundke, S. Pötting, J. Auxier, A. Schülzgen, N. Peyghambarian, N.F. Borrelli, Appl. Phys. Lett. 76 (2000) 10.
[14] V.G. Savitski, N.N. Posnov, P.V. Prokoshin, A.M. Malyarevich, K.V. Yumashev, M.I. Demchyk, A.A. Lipovskii, Appl. Phys. B 75 (2002) 841.
[15] A.M. Malyarevich, V.G. Savitsky, P.V. Prokoshin, N.N. Posnov, K.V. Yumashev, E. Raaben, A.A. Zhilin, JOSA B 19 (2002) 28.
[16] A. Dementjev, V. Gulbinas, L. Valkunas, I. Motchalov, H. Raaben, A. Michailovas, Appl. Phys. B 77 (2003) 595.
[17] J.L. Machol, F.W. Wise, R.C. Patel, D.D. Tanner, Phys. Rev. B 48 (1993) 2819.
[18] V. Liverini, S. Schön, R. Grange, M. Haiml, S.C. Zeller, U. Keller, Appl. Phys. Lett. 84 (2004) 4002.
[19] Z. Zhang, T. Nakagawa, K. Torizuka, T. Sugaya, K. Kobayashi, Appl. Phys. B 70 (2000) 59.
[20] S. Naumov, E. Sorokin, I. Sorokina, in: OSA Trends in Optics and Photonics, in: J.J. Zayhowski (Ed.), Advanced Solid-State Photonics, vol. 83, Optical Society of America, Washington, DC, 2003, p. 163.